

1 **Spatial modelling of the variability of the soil moisture regime at**
2 **the landscape scale in the southern Qilian Mountains, China**

3
4 C-Y. ZHAO ¹, P-C. QI ², Z-D. FENG ²
5
6

7 1 Key laboratory of arid and grassland agroecology (Ministry of Education), Lanzhou
8 University, Lanzhou 730000, China.

9 E-mail: nanzhr@lzb.ac.cn

10 2 Key laboratory of western China's environment systems (Ministry of Education),
11 Lanzhou University, Lanzhou 730000, China.

12 **Abstract**

13 The spatial and temporal variability of the soil moisture status gives an important base
14 for the assessment of ecological (for restoration) and economic (for agriculture)
15 conditions at micro- and meso-scales. It is also an essential input into many
16 hydrological processes models. However, there has been a lack of effective methods
17 for its estimation in the study area. The aim of this study was to determine the
18 relationship between the soil moisture status and precipitation and topographic factors.
19 First, this study compared a linear regression model with interpolating models for
20 estimating monthly mean precipitation and selected the linear regression model to
21 simulate the temporal-spatial variability of precipitation in the southern Qilian
22 Mountainous areas of the Heihe River Basin. Combining topographic index with the
23 distribution of precipitation, we calculated the soil moisture regime in the Pailugou
24 catchment, one representative comprehensive research catchment. The modeled
25 results were tested by the observed soil water content for different times. The

26 correlation coefficient between the modeled soil moisture status and the observed soil
27 water content is quite high, assuring our confidence in the spatially-modeled results of
28 the soil moisture status. The method was applied to the southern Qilian Mountainous
29 regions. Therefore the modeled distribution of the soil moisture status reflected the
30 interplay of the local topography and landscape climate processes. The driest sites
31 occur on some ridges in northern part and western part of the study area, where have
32 small accumulating flow areas and low precipitation rates. The wettest sites are
33 registered in the low river valley of the Heihe River and its major tributaries in the
34 eastern part due to large accumulating flow areas and higher precipitation rates.
35 Temporally, the bigger variation of the soil moisture status in the study occurs in July
36 and smaller difference appears in May.

37 **Keywords:** soil moisture status; precipitation; linear regression; topographic index;
38 Qilian Mountains; Landscape scale

39

40 **1 Introduction**

41 The Heihe River Basin, the second largest inland river basin in the arid regions
42 of northwestern China, consists of three major geomorphic units: the southern Qilian
43 Mountains, the middle Hexi Corridor, and the northern Alxa Highland. The southern
44 Qilian Mountains are hydrologically and ecologically the most important unit because
45 of the functions as the water source to support the irrigating agriculture in the Hexi
46 Corridor and also to maintain the ecological viability in the northern Alxa Highland.
47 With the rapid growth of population, agricultural irrigation areas increasingly spread

48 in the middle Hexi Corridor. As a result, the already-existing conflict between
49 economic use of the water here and ecological demand of the water in the Alxa
50 Highland has been recently exacerbated. How to resolve the conflict and coordinate
51 the development in economy and ecological environments becomes the focus of
52 attention in the Heihe River basin. Many researchers have dealt with water resources,
53 such as water resources carry capacity (Ji, et al., 2006), ecological requirement water
54 (Zhao, et al., 2005; Zhao et al., 2010), the runoff amount of the Heihe River and its
55 variation (Wang, et al., 2009), methods of irrigation and so on. The water resources
56 are very scarce in the Heihe River basin, and the runoff from the southern Qilian
57 Mountains approximately represents the water resources amount of the middle Hexi
58 Corridor and the northern Alxa Highland. Therefore, accurate estimation of runoff
59 from Qilian Mountainous watersheds is an urgent need for answering Heihe River
60 water resources carry capacity and for water management and planning. To
61 accomplish the needed runoff estimation in the upper reaches, several distributed
62 hydrological models are applied for the practical purpose. Soil moisture is considered
63 to be an important parameter in these distributed hydrology models. It thus has to be
64 spatially and temporally portrayed (Liang et al., 1994; Wignosta et al., 1994; Famiglietti
65 and Wood, 1994; Li & Islam, 1999). For the reason, during the last 30 years there
66 have been various studies that have attempted to develop a method to estimate the soil
67 moisture content over large scale. The one commonly used is extrapolation approach
68 in which one method is to estimate soil moisture by extrapolating point measurements
69 across the landscape with geostatistical techniques (Western and Grayson, 1998;

70 Wang et al., 2001;Western et al., 2004). Unfortunately, ground-based methods (e.g.
71 neutron thermalization, oven-dry method) are much too labor-intensive to maintain
72 for a large area (e.g., in the entire southern Qilian Mountains). Another method is to
73 estimate soil moisture by using wetness indices based on terrain information (e.g.
74 Beven and Kirkby, 1979; O'Loughlin, 1986; Svetlitchnyi et al., 2003; Teuling and
75 Troch, 2005). The latter method hypothesizes that the spatial distribution of
76 topographic attributes that characterize these flow paths inherently captures the spatial
77 variability of soil moisture status at the meso-scale as well. However, soil moisture
78 patterns are influenced by a number of factors such as soil properties, vegetation,
79 depth to water table and meteorological conditions besides topographic attributes.
80 Climate, parent material, topography, vegetation, and other biotic agents are the
81 dominant soil-forming process, but climate probably exert control at larger scales
82 (Moore et al., 1988; Gómez-Plaza et al., 2001). Thus, in this study the relationship of
83 the temporal and spatial variation of soil moisture is determined by establishing its
84 controlling factors, e.g. topography and precipitation. Topographic attributes can be
85 easily extracted from a digital elevation model (DEM). Whereas, precipitation fields
86 on a regular grid and in digital forms must be inferred from neighbouring
87 meteorological stations or from relationships with other variables (Marquínez et al.,
88 2003). There are many methods of interpolating precipitation from monitoring
89 stations to grid points (Dirks et al., 1998; Goovaerts, 2000; Wei, et al., 2005; Price et
90 al., 2000; Guenni & Hutchinson, 1998). Basic techniques use only the geographic
91 coordinates of the sampling points and the value of the measured variable. However,

92 the study area is one in which these methods have not been applied previously. In
93 addition, regression models are using only additional information as regression
94 models between precipitation and various topographic variables such as altitude,
95 latitude, continentality, slope, orientation or exposure (Basist et al., 1994; Goodale et
96 al., 1998; Ninyerola et al., 2000; Wotling et al., 2000; Weisse & Bois, 2001). But few
97 researchers could interpolate precipitation by regression models in the study area
98 because of unavailable digital elevation models (DEM). Fortunately, significant
99 progress in this area has recently been achieved through the development of a
100 high-resolution DEM with a resolution of 10m×10m by the remote sensing laboratory
101 of Cold and Arid Regions Environmental and Engineering Research Institute, CAS.
102 The topographic factors of soil moisture are best delineated by the DEM at the
103 resolution that closely matches the smallest orographic scale supported by the data.

104 This study sought to develop the relationships between soil moisture and its
105 controlling factors (i.e., precipitation and topographic variables) in order to map the
106 soil moisture status across the southern Qilian Mountains. In the following sections
107 we will present the various steps that lead to the mapping of the soil moisture regime:
108 (1) use of available data; (2) determination of the best model for modelling the areal
109 distribution of precipitation; (3) definition of the wetness index and GIS realization of
110 the wetness index model; (4) mapping of the soil moisture status distribution; and
111 finally (5) validation of the results.

112

113 **2 Materials and methods**

114 **2.1 Study area**

115 The study area, one portion of the Qilian Mountains within the Heihe River
116 Basin, is located between $98^{\circ} 34' - 101^{\circ} 11' E$ and $37^{\circ} 41' - 39^{\circ} 05' N$ and covers
117 an area of approximately $10,009 \text{ km}^2$, with the elevation ranging from 2000 to 5500m
118 a.s.l. Administratively, the major part of the study area is in Gansu Province and a
119 small part in Qinghai Province (Fig. 1). The mean annual precipitation increases with
120 the increasing elevation (from 250 to 700mm). The inter-annual variability in the
121 precipitation is as high as 80%, and over 88% of the precipitation falls between May
122 and September. Figure 2 shows the pattern of rainfall over the year in Zhamashike
123 meteorological station (one representative meteorological station in the study area).
124 The mean annual temperature decreases with the increasing elevation (from 6.2 to -
125 9.6°C). The vegetation distribution closely follows the temperature- and
126 precipitation-determined heat-water combinations in the Mountains. They are (from
127 low to high elevations): desert steppe, forest steppe, sub-alpine shrubby meadow,
128 alpine cold desert, and ice/snow zone. In addition to the obvious vertical zonality,
129 horizontal zonality also exists due to precipitation and air temperature differences from
130 the south to the north and from the east to the west. Generally, precipitation decreases
131 from the east to the west and increases from the north to the south but the temperature
132 is reverse in the study area.

133
134 Figure 1 Location of the study area, meteorological stations and rain gauges.
135
136

137 Figure 2 Distribution of monthly mean precipitation in Zhamashike meteorological
138 station (1957-1995).

139 2.2 Data collection

140 The monthly mean precipitation data (from 1957 to 1995) were obtained from 43
141 stations, including meteorological stations and rain gauges located within the study
142 area and the surrounding areas. The locations and the altitudes of these stations were
143 measured with a global positioning system (GPS) and an elevation meter. Among
144 them, 30 stations were chosen to develop the regression model or to use for
145 interpolating and other 13 stations were remained to test the models. Total 27 plots
146 were located to measure soil water content, 22 plots were in Pailugou catchment (one
147 representative comprehensive research catchment in the study area located at 38.55° N,
148 100.30° E) (Fig. 1). Pailugou catchment covers an area of 10 km², with the elevation
149 ranging from 2600m to 3800m a.s.l. Soil was sampled on a biweekly interval at four
150 depths (0-10, 10-20, 20-40, 40-60 cm) from May to September in 2003 and 2004. Soil
151 moisture was measured by the conventional oven-dry method. Calculation of mean
152 value of soil water content (SWC) is demonstrated as follows: suppose that SWC of
153 plot i , layer j , sampling occasion k is expressed as $SWC_{i,j,k}$. N_j represents the number
154 of sampling soil layer or soil depths and is 4 in this study; N_k is the number of
155 sampling occasion in each month, which is 2. Mean SWC in each month on plot i
156 (SWC_i) is calculated as follows:

$$157 \quad SWC_i = \frac{1}{N_k \times N_j} \sum_{k=1}^2 \sum_{j=1}^4 SWC_{i,j,k} \quad (1)$$

158 At final, we can get available data of 15 plots, which was used to validate the model

159 mentioned hereinafter. Pailugou catchment has a weather station at the catchment
160 outlet. 16 rain gauges were located along elevation gradient, on a 100m interval
161 between 2600-3500m and on a 50m intervals between 3500-3800m, for providing
162 information on the spatial variability of rainfall.

163 DEMs of the study area and Pailugou catchment were obtained from the remote
164 sensing laboratory of Cold and Arid Regions Environmental and Engineering
165 Research Institute, CAS.

166 **2.3 Description of models**

167 Hydrological prediction at the micro- and meso-scales is intimately dependent on
168 the ability to characterize the spatial variability of the soil water content. However,
169 soil moisture exhibits drastic temporal and spatial variations even in a small
170 catchment. In mountainous terrains, the soil water distribution is controlled by vertical
171 and horizontal water divergence and convergence, infiltration recharge, and
172 evapotranspiration. The latter two terms are affected by solar insolation and the
173 vegetation canopy that vary strongly with exposure in arid areas. The
174 divergence/convergence term is dependent on hill-slope position (Moore et al., 1993).
175 Considering the hill-slope position, most index approaches for predicting the spatial
176 distribution of soil water can be expressed as (Beven and Kirkby, 1979):

$$177 \quad \quad \quad IN_I = \ln (\alpha / \tan \beta) \quad \quad \quad (2)$$

178 where IN_I is the wetness index, α the contributing area and β the local slope of the
181 terrain. The soil water content is not only affected by the divergence/convergence of
182 water but also affected by evapotranspiration. In arid areas, evapotranspiration is

183 obviously different in different aspects because of variations of insolation. A modified
184 wetness index is defined by merely introducing the factor of aspect (A), an appropriate
185 surrogate of potential insolation (Grayson et al., 1997; Gomez-Plaza et al., 2001).
186 Then, the Eq.(2) becomes:

187

$$188 \quad IN_2 = \ln(a/\tan \beta) \times \cos A \quad (3)$$

189

190 where IN_2 is the modified wetness index and A the aspect.

191 The soil moisture index at landscape scales is determined by high-resolution
192 spatial distributions of precipitation and DEM-based topographic factors (Dymond
193 and Johnson, 2002) and given as the following:

194

$$195 \quad IN_3 = \ln(a/\tan B) \times \cos A \times P_i \quad (4)$$

196

197 where IN_3 is the soil moisture index in every month, P_i the monthly mean precipitation.

198 Eq.(4) requires four parameters: slope, aspect, the specific catchment area (catchment
199 area draining across a unit width of contour) and precipitation. Topographical
200 parameters such as slope (β), aspect (A), and the contributing area (α) are computed
201 from DEM. Precipitation is an important parameter and must be accurately estimated.

202 The temporal and spatial distribution of precipitation in Pailugou catchment was
203 simulated by regression relationship between the monthly mean rainfall and altitude,
204 which is presented as:

$$205 \quad P_i = a + bH + cH^2 \quad (5)$$

206 where H is the altitude in meter, a , b and c the regression coefficients (Table 1)

207 We here used five methods to simulate the temporal and spatial distribution of
208 precipitation in the southern Qilian Mountains, i.e. linear regression, inverse distance
209 weighted (IDW), ordinary kriging (OK), trend and spline. The regression model
210 derived by regression analyses can predict annual, monthly precipitation as functions
211 of elevation and geographical coordinates (Wei et al., 2005; Michaud et al., 1995). By
212 the analysis of the precipitation data with their elevation and geographical coordinates
213 in the study, a linear regression relationship between the monthly mean rainfall and
214 locational/topographic factors is presented as:

$$P_i = a + bH + cY + dX \quad (6)$$

218 where H is the altitude in meter, Y the latitude in degree, X the longitude in degree and
219 a , b , c , d the regression coefficients (Table 2).

220

Table 1

221

Table 2

222

223 Besides the regression model, four conventional interpolation methods, inverse
224 distance weighted (IDW), spline, ordinary kriging (OK), and trend, were tested. IDW
225 estimates the value of an unsampled area as a weighted average of a defined number
226 of neighborhood points, or area, and the weight assigned to each neighborhood point
227 diminishes as the distance to the neighborhood point increases (Lloyd, 2005). Spline
228 interpolators have been widely used in developing climatic surfaces from sparse
229 observation points (Tsanis and Gad, 2001). The interpolated surface based on spline

230 (a) passes exactly through the data points and (b) has a minimum curvature. OK is a
231 geostatistical procedure that uses a variogram model, which describes the spatial
232 continuity of the input data to estimate values at unsampled locations (Isaaks and
233 Srivastava, 1989). The variability between samples as a function of distance (i.e.,
234 semivariance) is evaluated and modeled prior to kriging (Wackernagel, 1995). The
235 trend surface interpolator uses a polynomial regression to fit a least-squares surface to
236 the input points. It creates smooth surfaces. The surface generated will seldom pass
237 through the original data points since it performs the best fit for the entire surface.

238 **3 Results and discussion**

239 **3.1 Wetness indexes**

240 Topographical parameters, such as slope, aspect and the contributing area were
241 computed from DEM. The aspect is expressed in positive degrees from 0 to 360,
242 measured clockwise from the north. The maps of the wetness index (IN_1 and IN_2) and
243 the modified wetness index (IN_3) in Pailugou catchment were obtained from the
244 models using ARC/INFO + grid. The simulated wetness indexes were validated by
245 observed data. We found that IN_1 was able to explain between 34% and 38% of the
246 spatial variability of soil moisture, but if the aspect was considered as a
247 complementary factor, this capacity increased up to 69.5%. The results were
248 supported by some researches (Moor et al., 1988; Gómez-Plaza et al., 2001). However,
249 Eq. (2) and Eq. (3) only take the topographic factors into account. If the spatially
250 inhomogeneous precipitation was considered as another complementary factor (i.e. Eq.
251 (4)), the capacity of the spatial variability of soil moisture can be explained to be 76%

252 in Pailugou catchment (Fig. 3). The maps of the wetness index (IN_1) and the modified
253 wetness index (IN_2) in the southern Qilian Mountains were obtained from the models
254 using ARC/INFO + grid (Fig. 4). According to precipitation measurement,
255 precipitation shows dramatically differences in the southern Qilian Mountains. It
256 increases from the north to the south, from the lower altitude to the higher altitude,
257 and decreases from the east to the west. In turn, the soil moisture status exhibits a
258 spatially inhomogeneous arrangement in the landscape due to precipitation. Therefore,
259 precipitation must be considered.

260 Figure 3 Scatter plots of observed soil moisture content and modeled soil moisture
261 status from May to August

262 Figure 4 Distribution of wetness indexes (IN_1 and IN_2) in the southern Qilian
263 Mountains.

264 **3.2 Spatial and temporal distributions of precipitation**

265 Prediction of precipitation on the locations of the validation points and the
266 measured values at these locations were compared by three criteria: the mean error
267 (ME), the mean absolute error (MAE) and the root mean square error (RMSE). ME
268 indicates the degree of bias, MAE provides a measure of how far the estimate can be
269 in error, ignoring the sign, and RMSE provides a measure that is sensitive to outliers.
270 A summary of the errors obtained from the criteria was presented in Table 3. ME was
271 relatively low for IDW, OK, trend and linear regression, but was generally lowest for
272 the linear regression model. The linear regression and OK methods gave the lower
273 MAE and RMSE. The spline gave consistently poor performances. For five methods,

274 there were substantial variations in RMSE through the year (Fig. 5). The highest
275 errors occurred from July to September and the lowest values from October to
276 February, which probably reflected the greater precipitation differences across the
277 region in summer. From June to August, the linear regression performed better than
278 OK. Thus the conclusions are as follows: on average over the year, larger predictions
279 errors were obtained by the spline, the trend and IDW methods that ignore elevation
280 factors, with the worst results produced by the spline. It was noteworthy that for
281 several months (from January to May, from September to December), OK yielded
282 smaller prediction errors than the linear regression of precipitation against elevation
283 and locational/topographic factors.

284 Table 3

285 Figure 5 Validation RMSE for monthly mean precipitation averaged across 13 test
286 stations for five methods.

287 As mentioned above, over 88% of the precipitation falls between May and
288 September and over 63% between June and August in the southern Qilian
289 Mountainous areas of the Heihe River Basin. We were here focusing on the spatial
290 distribution of precipitation during the ecologically meaningful time period, i.e.,
291 growing seasons approximately from May to August. Our comparison between these
292 models' performances demonstrated that the linear regression model did the best job
293 during the ecologically meaningful time period. The best performance of the linear
294 regression in the study area made this model the best choice. A series of
295 spatial-distribution maps of precipitation were obtained by the regression model (Fig.

296 6). Figure 6 showed that lower precipitation values were registered in the low valleys
297 of the Heihe River and the northwest part, and higher precipitation values appeared in
298 the southeast part where the altitude and longitude depended precipitation is higher.
299 Figure 6 also showed that precipitation value had temporal variations during growing
300 seasons (i.e. from May to August), highest precipitation value, ranging from 46mm to
301 145.4mm, appearing in the July, and the lowest precipitation value, from 25.2mm to
302 64.5 mm, being seen in May.

303 Figure 6 Distribution of monthly mean precipitation in southern Qilian Mountains
304 from May to August.

305 **3.3 Temporal and spatial distribution of soil moisture status in the southern** 306 **Qilian Mountains.**

307 The soil moisture data are fairly sparse in the study area. We could not collect the
308 soil moisture data except in Pailugou catchment. The soil moisture status of Pailugou
309 catchment was simulated using Eq.(4). To test the spatially-modeled results of the soil
310 moisture status in the catchment, we compared the observed results for 4 months at 15
311 sample plots with the spatially-modeled results for the corresponding months and
312 sample plots. The correlation coefficients (R^2) are from 0.60, 0.76, 0.67, 0.69 for May,
313 June, July and August respectively (Fig. 3). These assure our confidence in the spatial
314 model (i.e. Eq.(4)) of the soil moisture status.

315 Therefore, the same strategies were employed to estimate the soil moisture status
316 of the southern Qilian Mountains areas (Fig. 7). The distributions of the soil moisture
317 status in the study area reflected the interplay of the local and landscape climate

318 processes. As viewed from a small scale, the gentle bases of long hill-slopes had more
319 moisture than the steep short sites due to its larger catchment areas, and the
320 south-facing slope had less moisture than the north-facing slope because it got more
321 insolation on the dryness of the matrix soil water. From the landscape scale viewpoint,
322 the moisture increased from the north to the south and from the west to the east due to
323 the precipitation increase. Figure 7 showed that the driest sites (IN_3 from -1412 to
324 -985) occurred on some ridges in the northern part and the western part of the study
325 area, which has very small catchment areas and small precipitation. The wettest sites
326 (IN_3 from 1150 to 1577) were registered in the low valleys of the Heihe River and its
327 major tributaries in the eastern part due to large accumulating flow areas and more
328 precipitation. The bigger variation of the soil moisture status in the study occurred in
329 July and smaller difference appeared in May. Although there is temporal different in
330 the status of soil moisture, the spatial variation trend of soil moisture in different
331 month is the same. Comparing the dominant communities at 35 sample points
332 extracted from the present distribution of vegetation types with the spatially-modeled
333 results of soil moisture in June for the corresponding sample points (Table 4), we
334 found a certain community occupies its special range of soil moisture. For example,
335 Qinghai spruce (*Picea crassifolia*), distributing north-facing slope in the Qilian
336 Mountains, dominates the range of soil moisture (NI_3) between 0-800. *Stipa*
337 *breviflora*-*Stipa bungeana* has a range of soil moisture between -100-600 with higher
338 frequency between -100-200. *Stipa przewalskyi*-*Stipa purpurea* community covers a
339 range of soil moisture between -100-700 with higher frequency between 200-600.

340 *Salix gilasnanica* dominates a range between 300-1200, distributing above the upper
341 line of Qinghai spruce forest on the north-facing slope. *Kobresia tibetica* is dominant
342 species of the alpine meadow in Qilian Mountains. which occupies higher range of
343 soil moisture between 500-1400 with higher frequency between 800-1100.

344 Figure 7 Distribution of monthly mean soil moisture status in southern Qilian
345 Mountains from May to August.

346 Table 4 A range of soil moisture (NI_3) in five plant communities in southern Qilian
347 Mountains

348 In addition to topography, the land use type is another important factor
349 controlling soil water patterns, which means that difference in vegetations resulting
350 from different land use types was one of the major factors influencing soil moisture
351 variability. However, the factor of vegetations is not included in Eq. (4). How to
352 improve the model to estimate the soil moisture status is an objective of our future
353 study.

354

355 **4 Conclusions**

356 Accurate prediction of the soil moisture status at the large scale is of crucial
357 interest to hydrology and agronomy related studies in the southern Qilian Mountains.
358 However, soil moisture data are not available and ground-based methods (e.g. neutron
359 thermalization, oven-dry method) are far too labor-intensive to maintain for the large
360 area (e.g., the entire southern Qilian Mountains). Therefore, it is very important to
361 develop more descriptive models of the soil moisture status. We can draw some

362 conclusions from the approach:

363 1. Equation (4) was used to predict the variability of the soil moisture status in
364 the study area and the model was validated by Pailugou catchment. The results of
365 validation assured our confidence in the spatially-modeled results of the soil moisture
366 status. But one important factor affecting soil moisture is vegetation types which were
367 excluded in the model. Vegetation, which is in part responsible for the distribution of
368 soil moisture, will be integrated in equation (4) to improve the estimation accuracy in
369 future work. Further studies would benefit from using these types of index to set up
370 the distributed initial soil water conditions in the hydrological modeling of the study
371 area incorporating estimated evapotranspiration fluxes of vegetation.

372 2. Equation (4) includes two terms, the topographic indices and precipitation.
373 The model of the topographic indices in Eq. (3) is universal in a different sense.
374 Therefore accurate estimations of precipitation are very important to estimate the soil
375 moisture state at large scale. We selected five methods to simulate the temporal-spatial
376 distributions of precipitation in the study. By comparison, the best performance of the
377 linear regression in the study area made this model the best choice.

378 3. Soil moisture status is influenced by other factors, such as soil properties,
379 vegetation, meteorological conditions besides topography. The importance of these
380 factors can vary with the study area. Any simple relationship between topographic
381 indices and soil moisture must, however, be used with great care (Rodhe and Seibert,
382 1999; Svetlitchnyi et al., 2003). According to Florinsky et al. (2002) in soil studies
383 with digital terrain modelling, there is a need to take into account four types of

384 variability in relations between soil and a relief: regional, time, depth, and scale. For
385 example, Chinese Loess Plateau comparing with the southern Qilian Mountains, three
386 natural factors: steeply-sloped topography with gullies, fine-textured loessial soils and
387 precipitation in form of storms are first and foremost considered. These factors decide
388 the unique hydrogeomorphic condition that the rainfall intensity often exceeds the soil
389 infiltration capacity differing from that in the southern Qilian Mountains. This
390 imposes on equation (4) quite certain regional restrictions.

391

392 **Acknowledgements**

393 This project was supported by Nation Natural Science Foundation of China
394 (No. 30770387, No. 40671067); National Environmental Protection Commonweal
395 Project of China (NEPCP 200809098).

396 **References**

- 397 1. Basist, A., Bell, G. D., and Meentemeyer, V.: Statistical relationships between
398 topography and precipitation patterns, *J.Climat*, 7, 1305-1315, 1994.
- 399 2. Beven, K. J., and Kirkby, M. J.: A physically based, variable contributing area
400 model of basin hydrology, *Hydrological Science Bulletin*, 24, 43-69, 1979.
- 401 3. Dirks, K. N., Hay, J. E., Stow, C. D., and Harris, D.: High-resolution studies of
402 rainfall on Norfolk Island part II: interpolation of rainfall data, *J. Hydrol.*, 208,
403 187-193, 1998.
- 404 4. Dymond, C. C., and Johnson, E. A.: Mapping vegetation spatial patterns from
405 modeled water, temperature and solar radiation gradients, *Journal of*
406 *Photogrammetry and Remote Sensing*, 57, 69-85, 2002.
- 407 5. Famiglietti, J. S., and Wood, E. F.: Multiscale modeling of spatially variable water
408 and energy balance processes, *Water Resour. Res.*, 30, 3061-3078, 1994.

- 409 6. Florinsky, I. V., Eilers, R. G., Manning, G. R., and Fuller, L. G.: Prediction of soil
410 properties by digital terrain modelling, *Environ. Modelling and Software*, 17,
411 295-311, 2002.
- 412 7. Gómez-Plaza, A., Martínez-Mena, M., Albaladejo, J., and Castillo, V. M.:
413 Factors regulating spatial distribution of soil water content in small semiarid
414 catchments, *J. Hydrol.*, 253, 211-226, 2001.
- 415 8. Goodale, C. L., Alber, J. D., and Ollinger, S. V.: Mapping monthly precipitation,
416 temperature and solar radiation for Ireland with polynomial regression and digital
417 elevation model, *Clim. Res.*, 10, 35-49, 1998.
- 418 9. Goovaerts, P.: Geostatistical approach for incorporating elevation into the spatial
419 interpolation of rainfall, *J. Hydrol.*, 228, 113-129, 2000.
- 420 10. Grayson, R. B., Western, A. W., and Chiew, F. H. S.: Preferred states in spatial soil
421 moisture pattern: local and nonlocal controls, *Water Resour. Res.*, 33, 2879-2908,
422 1997.
- 423 11. Guenni, L., and Hutchinson, M. F.: Spatial interpolation of the parameters of a
424 rainfall model from ground-based data, *J. Hydrol.*, 212-213, 335-347, 1998.
- 425 12. Isaaks, E. H., and Srivastava, R. M.: An introduction to applied geostatistics,
426 Oxford University Press, New York, 516pp., 1989.
- 427 13. Ji, X. B, Kang, E., and Chen R. S.: Analysis of Water Resources Supply and
428 Demand and Security of Water Resources Development in Irrigation Regions of
429 the Middle Reaches of the Heihe River Basin, Northwest China, *Agricultural
430 Sciences in China*, 5, 130-140, 2006.
- 431 14. Li J. K., and Islam S.: On the estimation of soil moisture profile and surface fluxes
432 partitioning from sequential assimilation of surface layer soil moisture, *J. Hydrol.*,
433 220, 86-103, 1999.
- 434 15. Liang, X., Lettenmaier, D. P., Wood, E. F., and Burges, S. J.: A simple
435 hydrologically based model of land surface water and energy fluxes for general
436 circulation models, *J. Geoph. Res.*, 99, 14, 415-428, 1994.
- 437 16. Lloyd, C. D.: Assessing the effect of integrating elevation data into the estimation
438 of monthly precipitation in Great Britain, *J. Hydrol.*, 308, 128-150, 2005.

- 439 17. Marquínez J., Lastra J., and García P. : Estimation models for precipitation in
440 mountainous regions: the use of GIS and multivariate analysis, *J. Hydrol.*, 270,
441 1-11, 2003.
- 442 18. Michaud, J. D., Auvine, B. A., and Penalba, O. C.: Spatial and elevation variations
443 of summer rainfall in the southwestern United States, *J. Appl. Meteorol.*, 34,
444 2689-2703, 1995.
- 445 19. Moore I. D., Turner A. K., Wilson J. P., Jenson S. K., and Band L. E.: GIS and
446 land-surface-subsurface process modeling. In: Goodchild M. F., Parks B. V.
447 Steyaert L. T. (eds) *Environmental modeling with GIS*. New York. pp 196-229,
448 1993.
- 449 20. Moore, I. D., Burch, G. J., and Mackenzie, D. H.: Topographic on the distribution
450 of surface soil water and the location of ephemeral gullies, *Trans. Am. Soc. Agric.*
451 *Eng.*, 31, 1098-1107, 1988.
- 452 21. Ninyerola, M., Pons, X., and Roure, J. M.: A methodological approach of
453 climatological modelling of air temperature and precipitation through GIS
454 techniques, *Int. J. Climatol.*, 20, 1823-1841, 2000.
- 455 22. O'Loughlin, E.M.: Prediction of surface saturation zones in natural catchments
456 by topographic analysis, *Water Resour. Res.*, 22, 794-804, 1986.
- 457 23. Price D. T., McKenney D. W., and Nalder I. A.: A comparison of two statistical
458 methods for spatial interpolation of Canadian monthly mean climate data, *Agr.*
459 *Forest Meteorol.*, 101, 81-94, 2000.
- 460 24. Rodhe, A. and Seibert J.: Wetland occurrence in relation to topography: a test of
461 topographic indices as moisture indicators, *Agricultural and Forest Meteorology*,
462 98-99, 325-340, 1999.
- 463 25. Svetlitchnyi, A. A., Plotnitskiy, S. V., and Stepovaya, O.Y.: Spatial distribution of
464 soil moisture content within catchments and its modelling on the basis of
465 topographic data, *J. Hydrol.*, 277, 50-60, 2003.
- 466 26. Teuling, A. J., and Troch, P. A.: Improved understanding of soil moisture
467 variability dynamics, *Geophys. Res. Lett.*, 32, L05404, 2005.
- 468 27. Tsanis, I. K., and Gad, M. A.: A GIS Precipitation method for analysis of storm

- 469 kinematics, *Environ. Modell. Softw.*, 16, 273-281, 2001.
- 470 28. Wackernagel, H.: *Multivariate Geostatistics*, Springer-Verlag, Berlin, 256pp,
471 1995.
- 472 29. Wang, J., Fu, B., Qiu, Y., Chen, L., and Wang, Z.: Geostatistical analysis of soil
473 moisture variability on Da Nangou catchment of the loess plateau, China, *Environ.*
474 *Geol.*, 41, 113-120, 2001.
- 475 30. Wang, J.S., Feng, J. Y., and Yang, L. F.: Runoff-denoted drought index and its
476 relationship to the yields of spring wheat in the arid area of Hexi corridor,
477 Northwest China, *Agricultural water management*, 96, 666-676, 2009.
- 478 31. Wei H., Li J., and Liang T.: Study on the estimation of precipitation resources for
479 rainwater harvesting agriculture in semiarid land of China, *Agr. Water Manage.*,
480 71, 33-45, 2005.
- 481 32. Weisse, A. K., and Bois, P.: Topographic effects on statistical characteristics of
482 heavy rainfall and mapping in the French Alps, *J. Appl. Meteorol.*, 40, 720-740,
483 2001.
- 484 33. Western, A., and Grayson, R.: The Tarrawarra data set: soil moisture patterns, soil
485 characteristics, and hydrological flux measurements, *Water Resour. Res.*, 34,
486 2765-2768, 1998.
- 487 34. Western, A., Zhou, S. L., Grayson, R. B., MacMahon, T. A., Bloschel, G., and
488 Wilson, D.: Spatial correlation of soil moisture in small catchments and its
489 relationship to dominant spatial hydrological processes, *J. Hydrol.*, 286, 113-134,
490 2004.
- 491 35. Wignosta, M. S., Vail, L. W., and Lettenmaier, D. P.: A distributed
492 hydrology-vegetation model for complex terrain, *Water Resour. Res.*, 30,
493 1665-1679, 1994.
- 494 36. Wotling, G., Bouvier, C., Danloux, J., and Fritsch, J. M.: Regionalization of
495 extreme precipitation distribution using the principal components of the
496 topographical environment, *J. Hydrol.*, 233, 86-101, 2000.
- 497 37. Zhao Chuanyan, Nan Zhongren, and Cheng Guodong: Methods for estimating
498 irrigation needs of spring wheat in the middle Heihe basin, China, *Agr. Water*

499 Manage., 75, 54-70, 2005.

500 38. Zhao, W. Z., Liu, B., and Zhang, Z. H.: Water requirements of maize in the
501 middle Heihe River basin, China, Agricultural water management, 97, 215-223,
502 2010.

503

504 Table 1. Monthly regression coefficients and R^2 needed to calculate monthly mean
505 precipitation using altitude (H) for Pailugou catchment ($P = a + bH + cH^2$).

time	a	b	c	R^2
Apr.	-0.00002	0.1344	-194.41	0.965
May	-0.00004	0.2386	-345.24	0.969
Jun.	-0.00020	0.9756	-1411.6	0.968
Jul.	-0.00010	0.7745	-1120.7	0.968
Aug.	-0.00005	0.3489	-504.77	0.967
Sep.	-0.00006	0.3770	-545.41	0.967

506

507

508 Table 2. Monthly linear regression coefficients and R^2 needed to calculate monthly
509 mean precipitation using altitude (H), latitude (Y) and longitude (X) for the southern
510 Qilian Mountains ($P = a + bH + cY + dX$).

time	a	b	c	d	R^2
Jan.	-19.811	0.000260	-0.051	0.231	0.207
Feb.	-70.701	0.001103	0.221	0.626	0.331
Mar.	-249.545	0.003390	0.433	2.336	0.406
Apr.	-16.862	0.004009	-4.289	1.879	0.584
May	408.331	0.009569	-12.540	0.869	0.810
Jun.	530.716	0.021000	-13.656	0.016	0.863
Jul.	689.699	0.029650	-12.485	1.018	0.870
Aug.	495.902	0.018520	-19.839	2.869	0.879
Sep.	196.940	0.009100	-15.049	4.003	0.856
Oct.	-5.170	0.002153	-5.737	2.341	0.841
Nov.	-136.015	0.000984	0.240	1.283	0.455
Dec.	-81.180	0.000480	0.493	0.627	0.166
Annual	1742.001	0.097260	-87.915	17.197	0.861

511

1 Table 3. Validation errors averaged across 13 test sites for the five interpolation methods in each month.

	Models	Jan	Feb	Mar	Apr	May	Jun	Jul	Aug	Sep	Oct	Nov	Dec
ME	IDW	0.20	0.95	2.56	0.83	-1.2	5.97	-2.58	1.28	-4.56	0.3	-0.68	0.59
	TREND	0.31	0.72	1.32	5.33	0.40	0.64	0.31	0.72	1.32	5.33	0.40	0.64
	OK	0.22	0.97	2.54	1.48	0.35	6.73	-2.23	2.66	-3.78	0.75	-0.65	0.58
	SPLINE	0.42	1.16	3.65	2.59	1.27	9.98	-0.94	4.5	-3.3	1.02	-0.38	0.7
	REGRESSION	0.32	1.04	2.3	0.36	-1.51	6.15	-3.56	-0.23	-6.09	-0.57	-0.75	0.7
MAE	IDW	0.84	1.56	4.46	5.34	6.84	11.41	12.68	9.98	6.47	3.1	1.52	1.15
	TREND	1.06	2.09	5.24	6.10	6.34	11.89	10.93	8.44	7.53	3.17	1.67	1.33
	OK	0.84	1.89	5	4.85	4.57	8.15	8.18	7.06	4.8	1.63	1.41	1.18
	SPLINE	0.97	1.81	7.29	6.99	7.04	12.18	12.57	9.71	6.68	2.79	1.51	1.47
	REGRESSION	1.05	1.98	4.94	5.86	5.03	7.46	6.07	4.6	7.41	2.92	1.72	1.3
RMSE	IDW	1.19	1.94	5.65	6.53	8.56	13.50	15.47	12.72	8.23	3.51	1.71	1.35
	TREND	1.28	2.22	8.13	8.88	8.52	15.01	15.80	10.52	8.23	3.88	1.88	1.79
	OK	1.18	2.16	6.16	6.21	5.54	10.78	9.75	8.62	6.05	2.18	1.65	1.37
	SPLINE	2.22	8.13	8.88	8.52	15.01	15.80	10.52	8.23	3.88	1.88	1.79	2.22
	REGRESSION	1.27	2.32	6.16	6.63	6.10	9.47	8.33	7.39	9.21	3.51	2.08	1.53

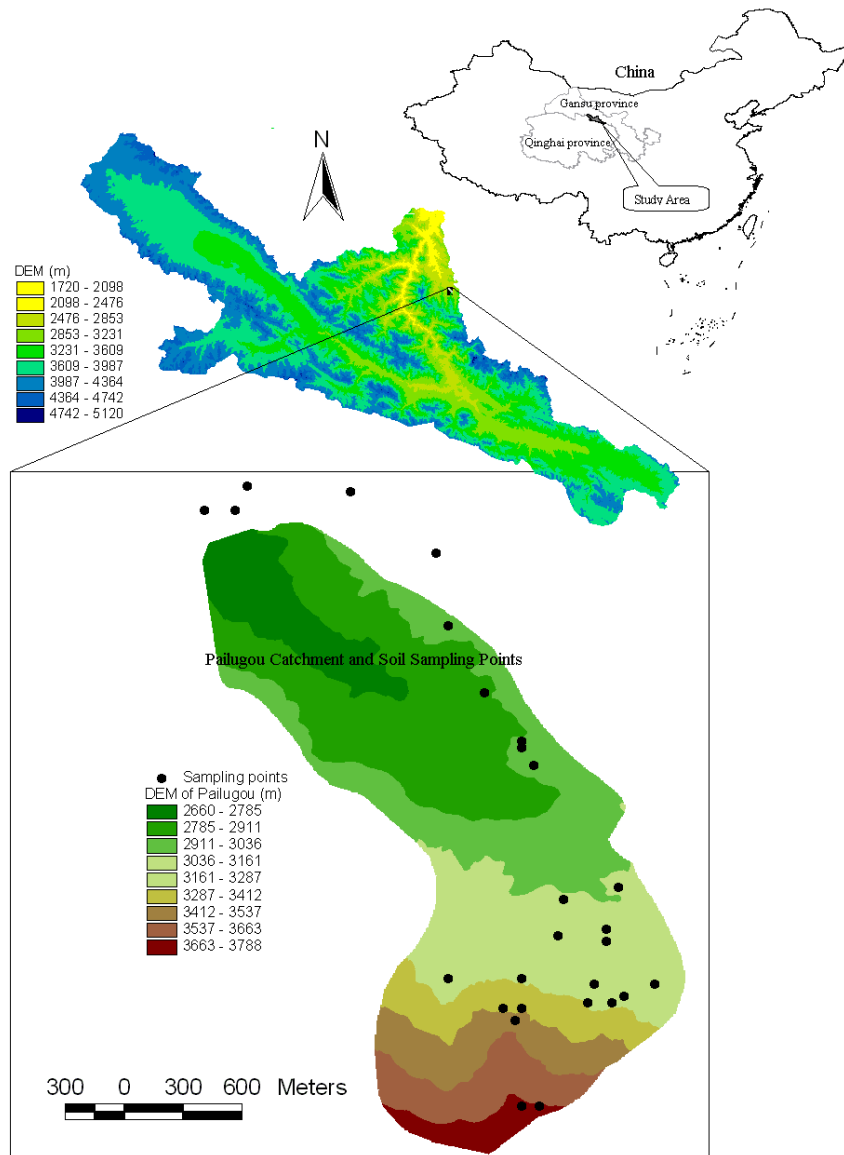
2

1 Table 4 A range of soil moisture (NI_3) in five plant communities in southern Qilian
 2 Mountains

NI_3 classes	Frequency of five communities				
	<i>Stipa breviflora</i> - <i>Stipa bungeana</i>	<i>Stipa przewalskyi</i> - <i>Stipa purpurea</i>	<i>Picea</i> <i>crassifolia</i>	<i>Salix</i> <i>gilasnanica</i>	<i>Kobresia</i> <i>tibetica</i>
-100-0	14.29	2.70	0.00	0.00	0.00
0-100	20.00	5.41	2.94	0.00	0.00
100-200	25.71	2.70	2.94	0.00	0.00
200-300	34.29	18.92	11.76	0.00	0.00
300-400	0.00	18.92	17.65	5.71	0.00
400-500	0.00	29.73	23.53	5.71	0.00
500-600	5.71	18.92	23.53	8.57	3.23
600-700	0.00	2.70	11.76	5.71	9.68
700-800	0.00	0.00	5.88	8.57	6.45
800-900	0.00	0.00	0.00	25.71	19.35
900-1000	0.00	0.00	0.00	25.71	19.35
1000-1100	0.00	0.00	0.00	5.71	22.58
1100-1200	0.00	0.00	0.00	8.57	9.68
1200-1300	0.00	0.00	0.00	0.00	6.45
1300-1400	0.00	0.00	0.00	0.00	3.23

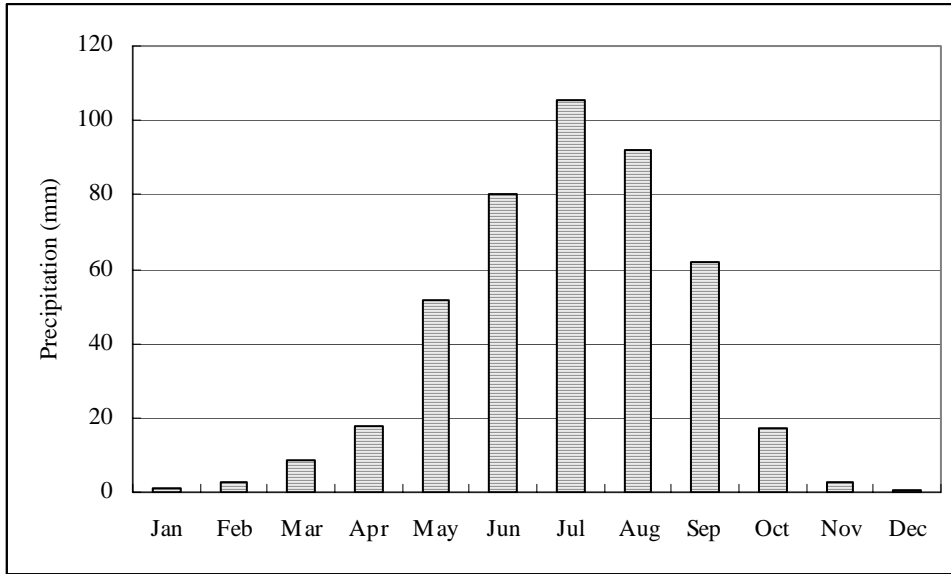
3

4



1
2
3
4
5
6

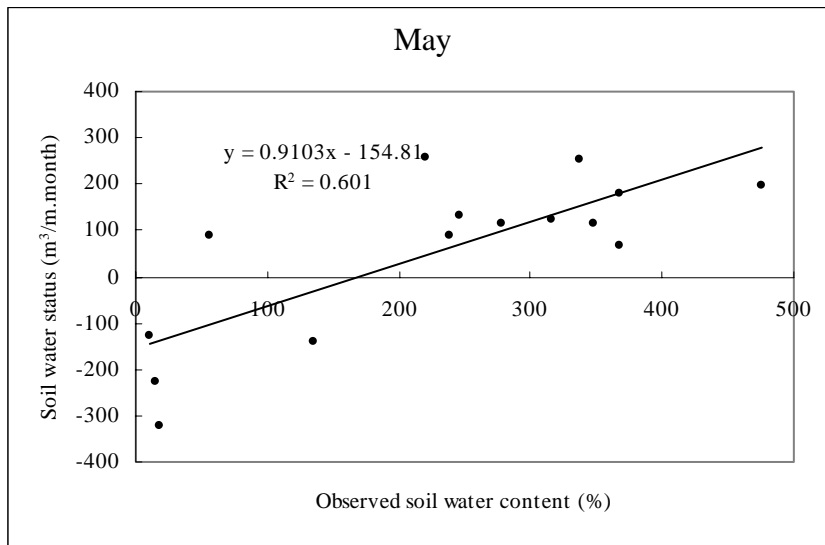
Figure 1. Location of the study area, meteorological stations and rain gauges in Pailugou catchment.



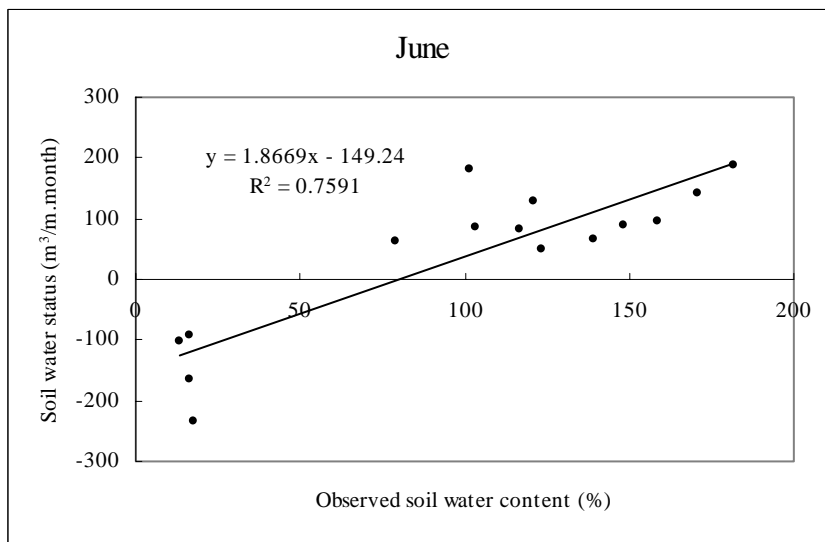
1
2
3
4
5
6
7
8
9
10
11
12
13
14
15
16
17
18
19
20
21
22
23
24
25
26
27
28
29
30

Figure 2. Distribution of monthly mean precipitation in Zhamashike meteorological station (1957-1995).

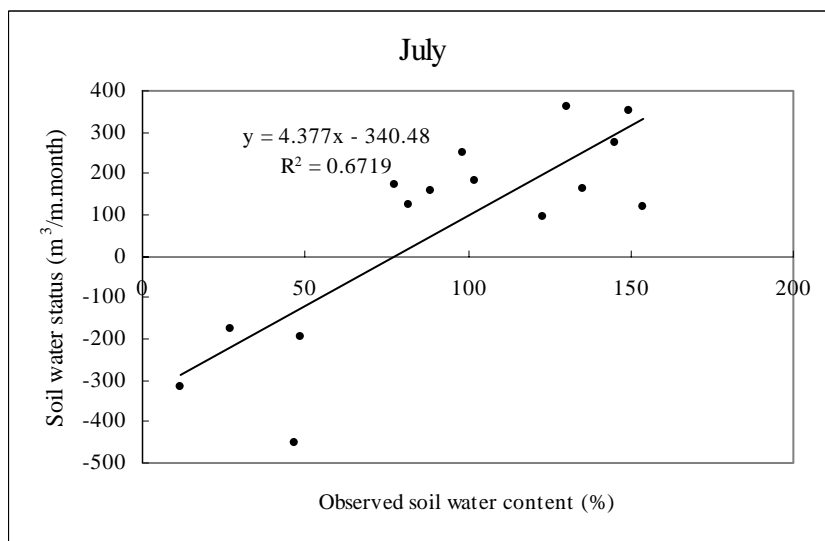
1



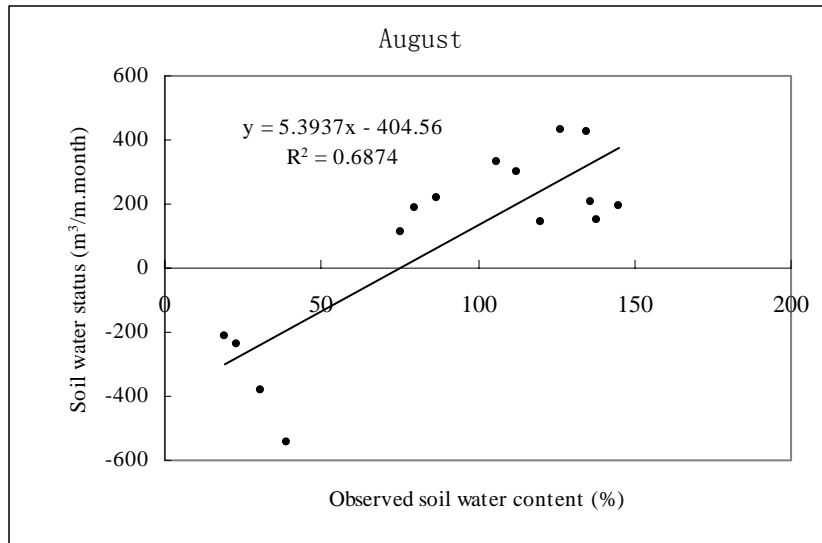
2



3

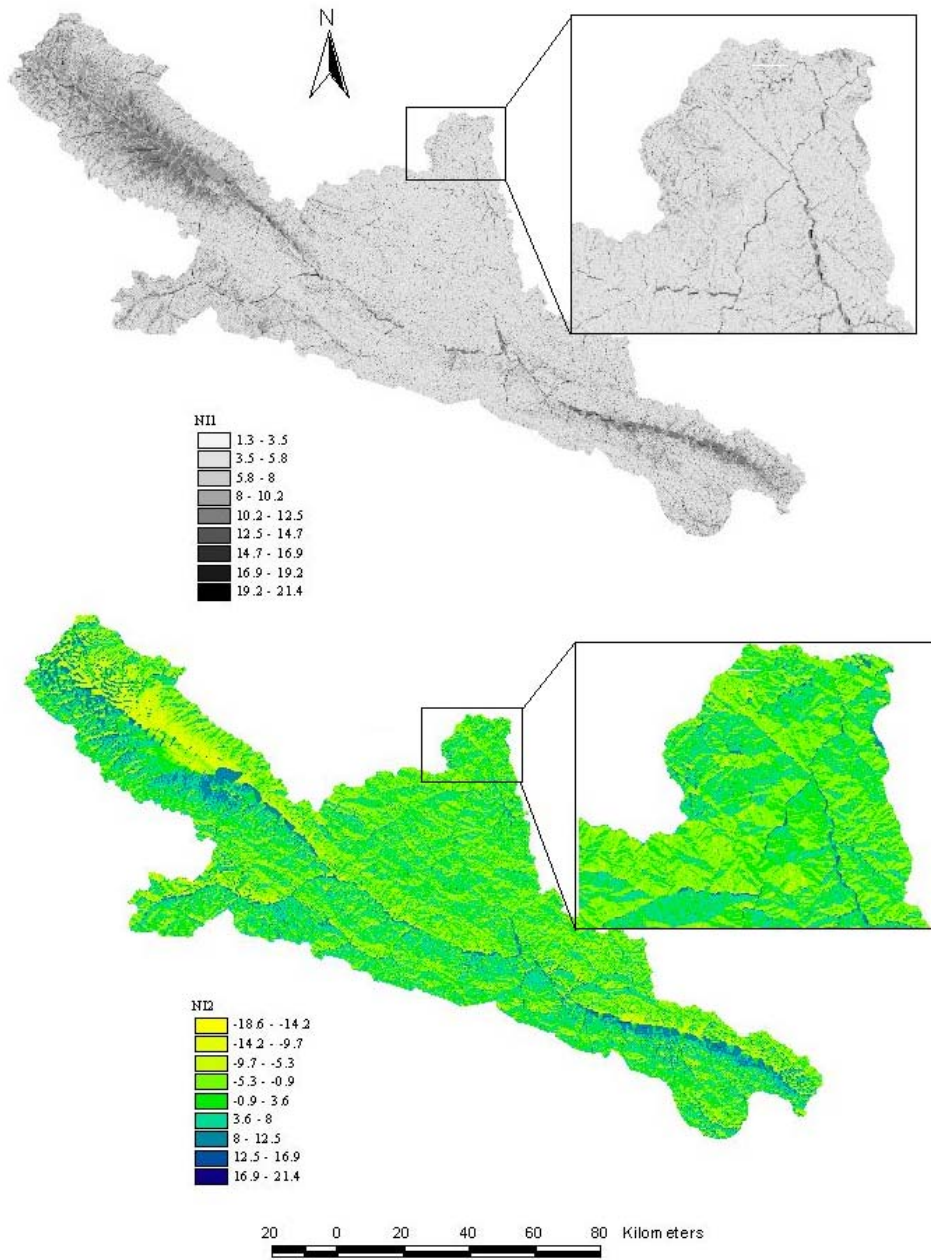


4



1
2
3
4
5
6
7
8
9
10
11
12
13

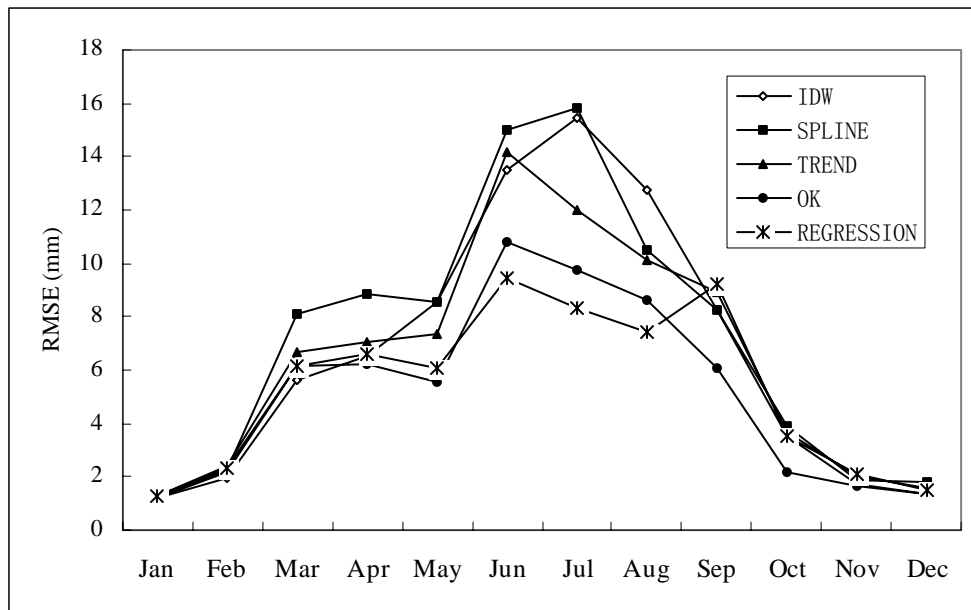
Figure 3. Scatter plots of observed soil moisture content and modeled soil moisture status from May to August



1
2
3
4
5
6
7
8
9
10
11
12

Figure 4. Distribution of wetness indexes (NI_1 and NI_2) in the southern Qilian Mountains.

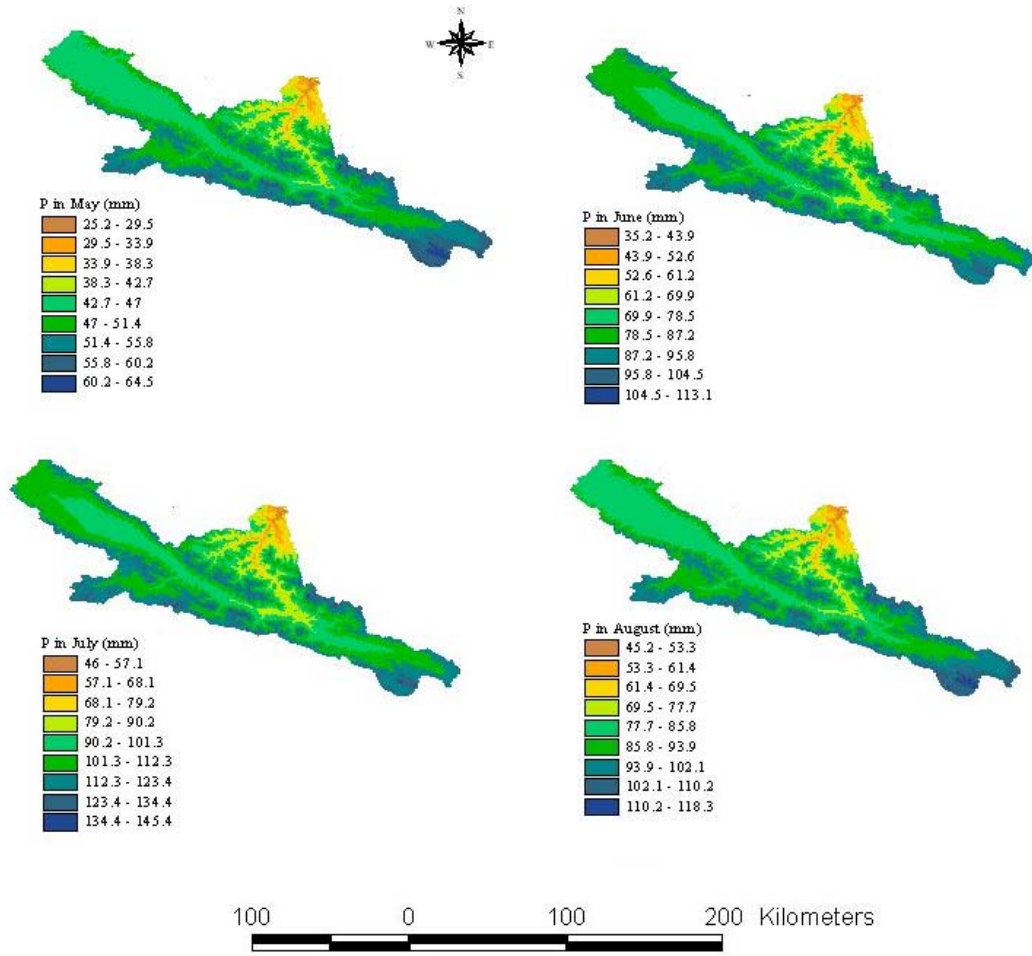
1
2



3
4
5
6
7
8
9
10
11
12
13
14
15
16
17
18
19
20
21
22
23

Figure 5. Validation RMSE for monthly mean precipitation averaged across 13 test stations for five methods.

1



2

3

Figure 6 Distribution of monthly mean precipitation in southern Qilian Mountains from May to August.

4

5

6

7

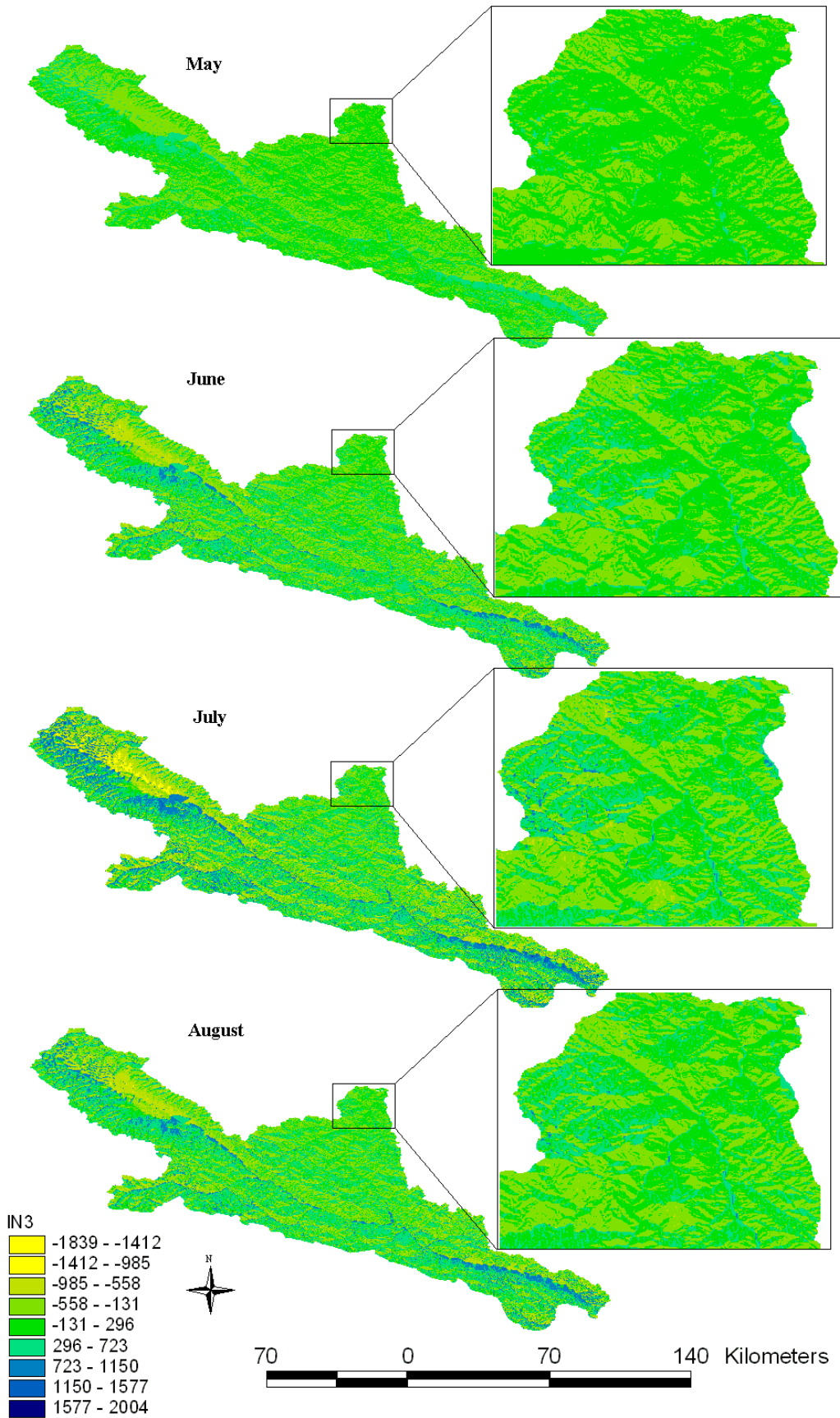
8

9

10

11

12



1
2
3

Figure 7. Distribution of monthly mean soil moisture status in southern Qilian Mountains from May to August.